Mn^{2+}/Mn^{4+} co-doped $LaM_{1-x}Al_{11-y}O_{19}$ (M = Mg, Zn) luminescent materials: electronic structure, energy transfer and optical thermometry properties

Dayu Huang,[a,b] Qiuyun Ouyang[a,*] Bin Liu,[a,b] Bingkun Chen,[a] Yuting Wang,[a] Chenggang Yuan,[a] Hui Xiao,[b] Hongzhou Lian,[b,*] and Jun Lin [b,*]

[a] *Key Laboratory of In-Fiber Integrated Optics, Ministry Education of China, and College of Physics and Opotoelectronic Engineering, Harbin Engineering University, Harbin 150001, China*

[b] *State Key Laboratory of Rare Earth Resource Utilization, Changchun Institute of Applied Chemistry, Chinese Academy of Sciences, Changchun 130022, P. R. China*

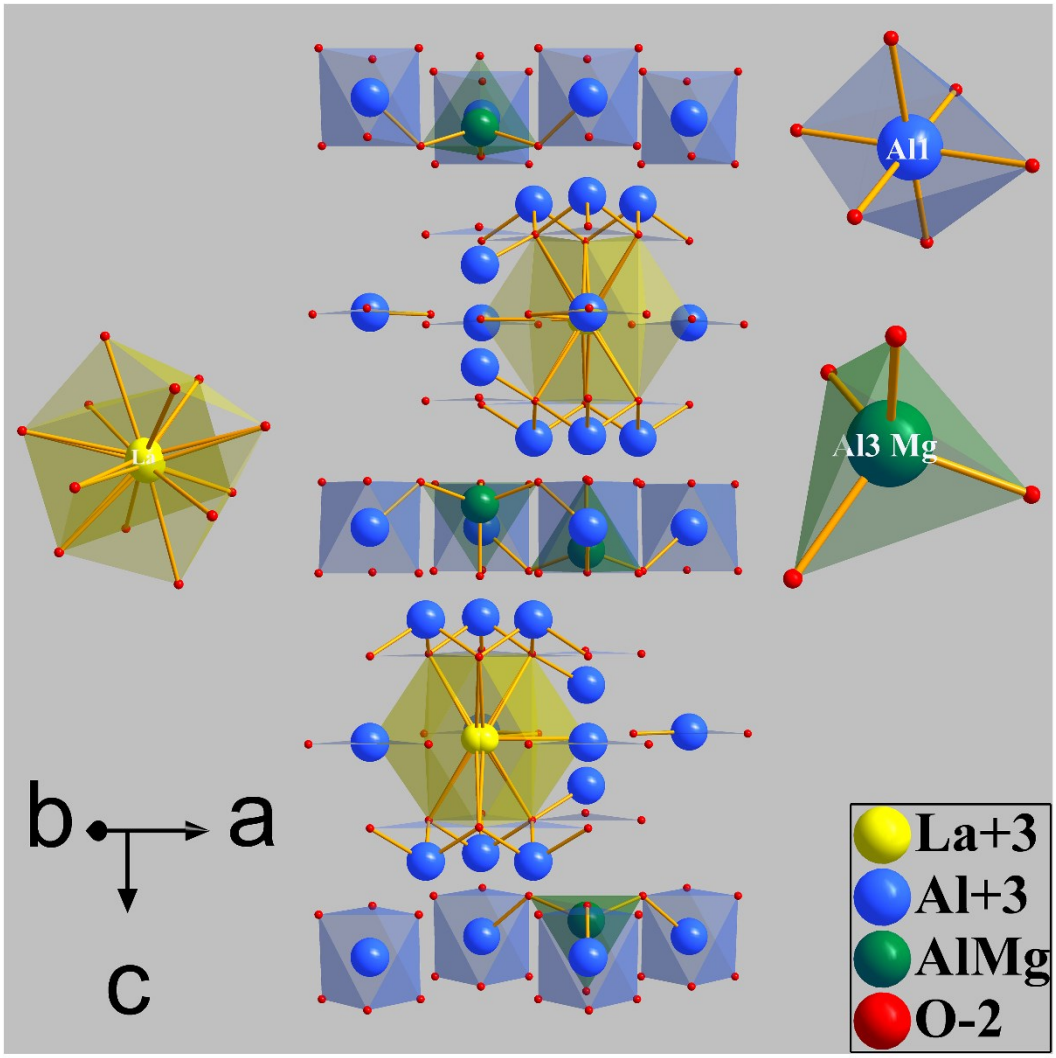

Figure S1. Unit cell of $LaZnAl_{11}O_{19}$ and the illustrated polyhedrons.

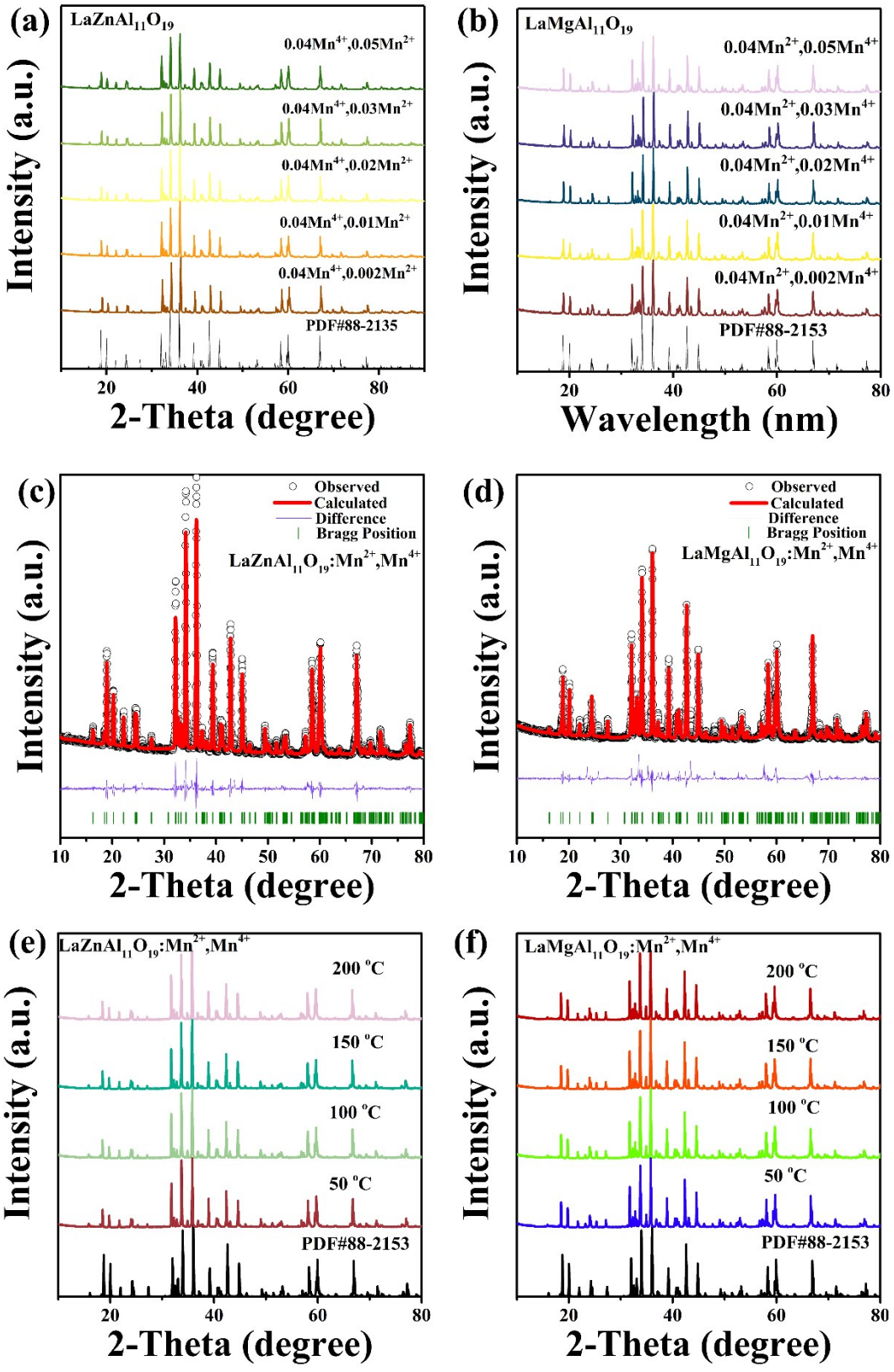

Figure S2. (a-b) Powder XRD patterns of $LaM_{1-x}Al_{11-y}O_{19}$:xMn^{2+},yMn^{4+} (M = Mg, Zn). Rietveld refinement XRD data of the representative (c) $LaZnAl_{11}O_{19}$:$0.04Mn^{2+}$,$0.03Mn^{4+}$, (d) $LaMgAl_{11}O_{19}$:$0.04Mn^{2+}$,$0.04Mn^{4+}$, (e-f) Powder XRD patterns of representative $LaM_{1-x}Al_{11-y}O_{19}$:$0.04Mn^{2+}$,yMn^{4+} (M = Mg, Zn) in the range of 50~200 °C.

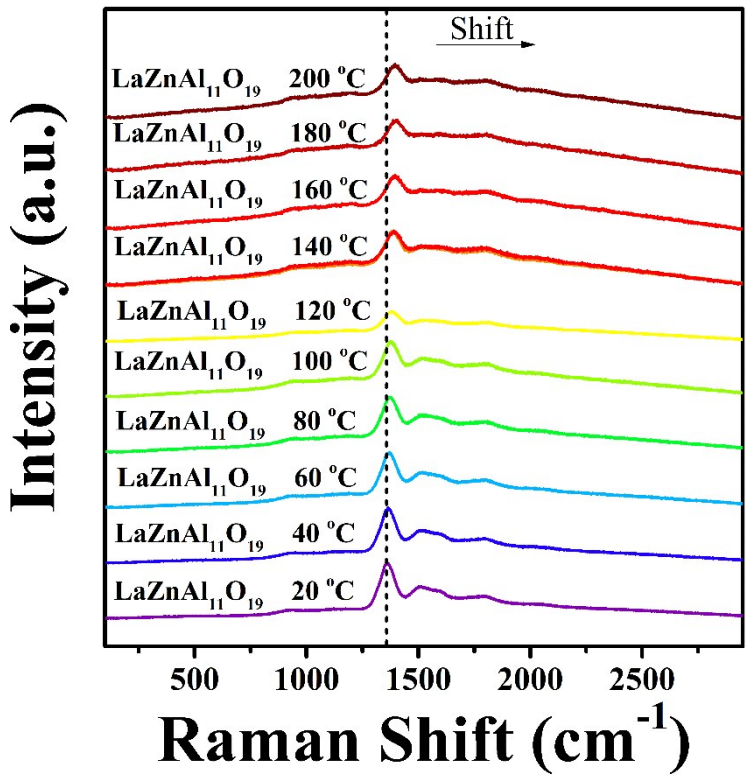

Figure S3. Temperature-dependent Raman spectra of $LaZnAl_{11}O_{19}$ in the 20-200 °C range.

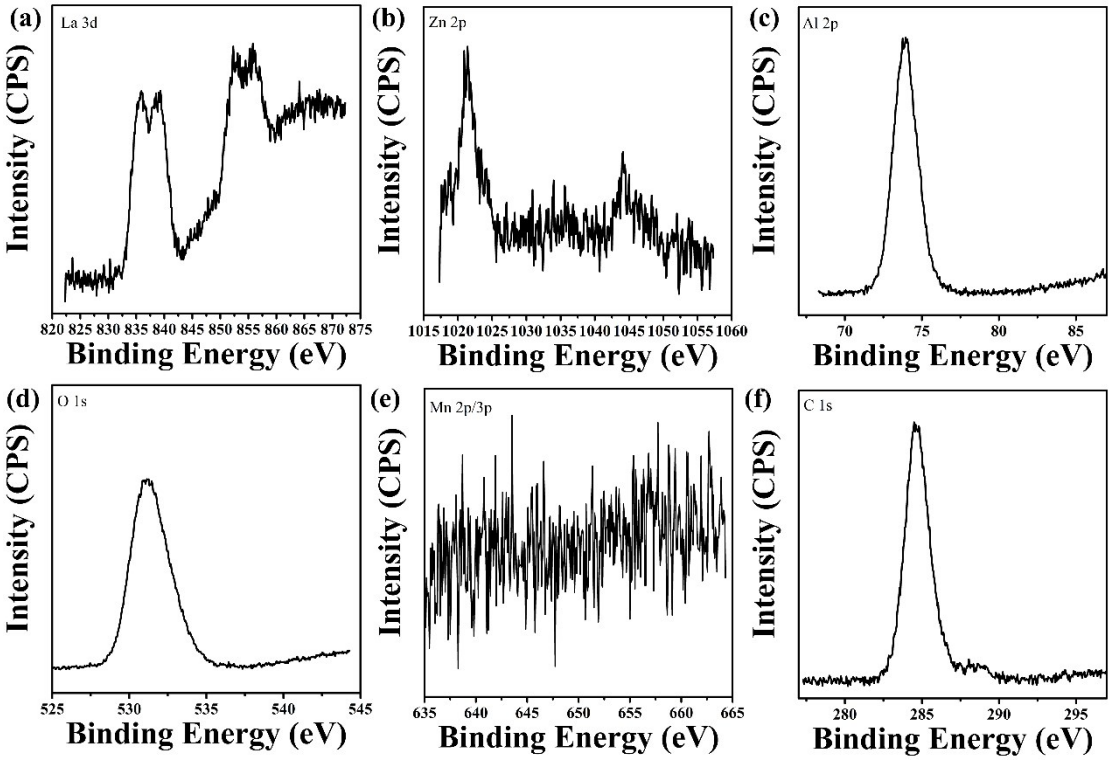

Figure S4. The La 3d, Zn 2p, Al 2p, O 1s, Mn 2p/3p and C 1s XPS spectra of $LaZnAl_{11}O_{19}:Mn^{2+},Mn^{4+}$.

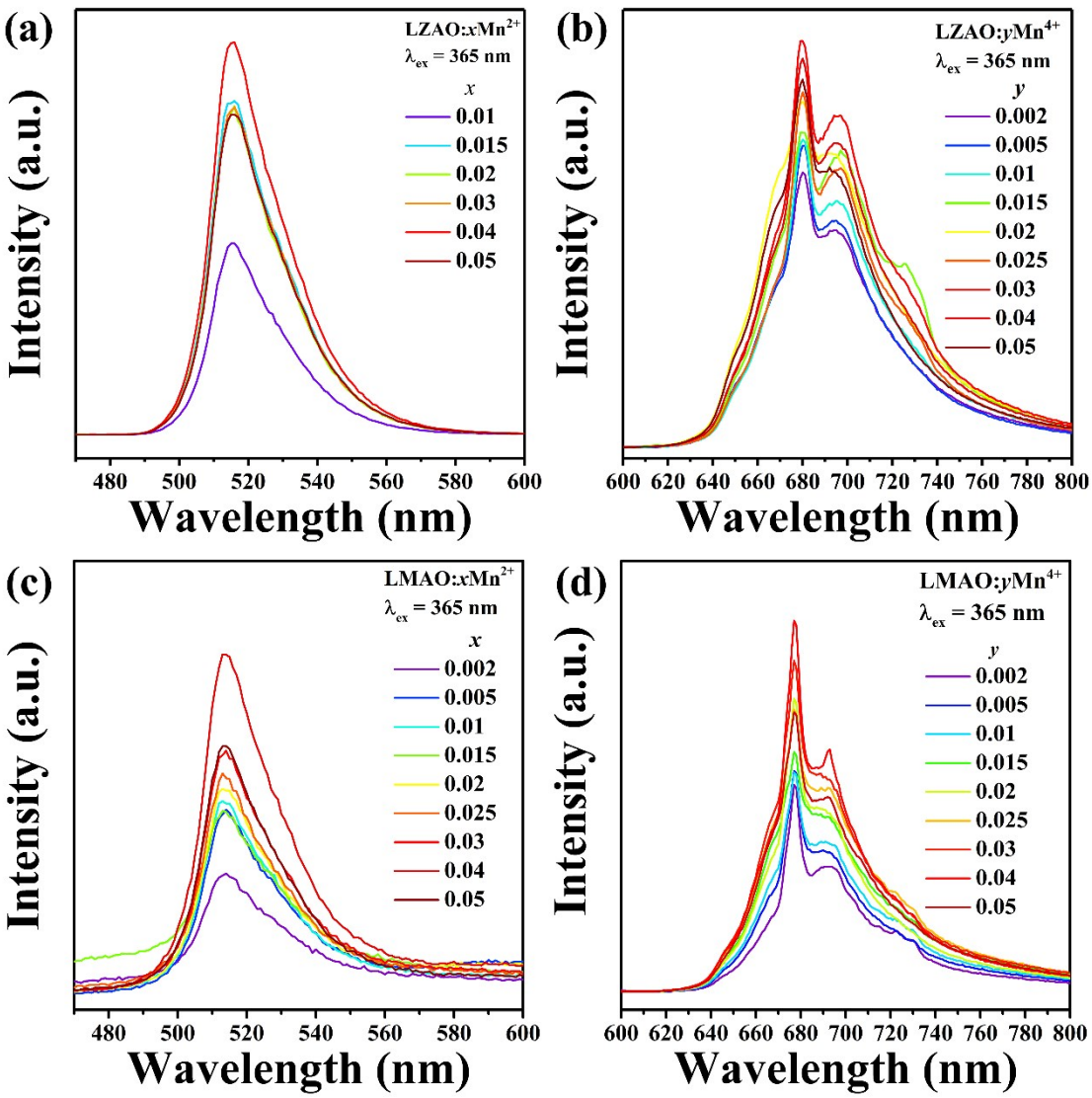

Figure S5. PL spectra of $LaZnAl_{11}O_{19}$ phosphors single-doped with (a) Mn^{2+} (λ_{ex} = 365 nm), (b) Mn^{4+} (λ_{ex} = 365 nm). PL spectra of $LaMgAl_{11}O_{19}$ phosphors single-doped with (c) Mn^{2+} (λ_{ex} = 365 nm), (d) Mn^{4+} (λ_{ex} = 365 nm).

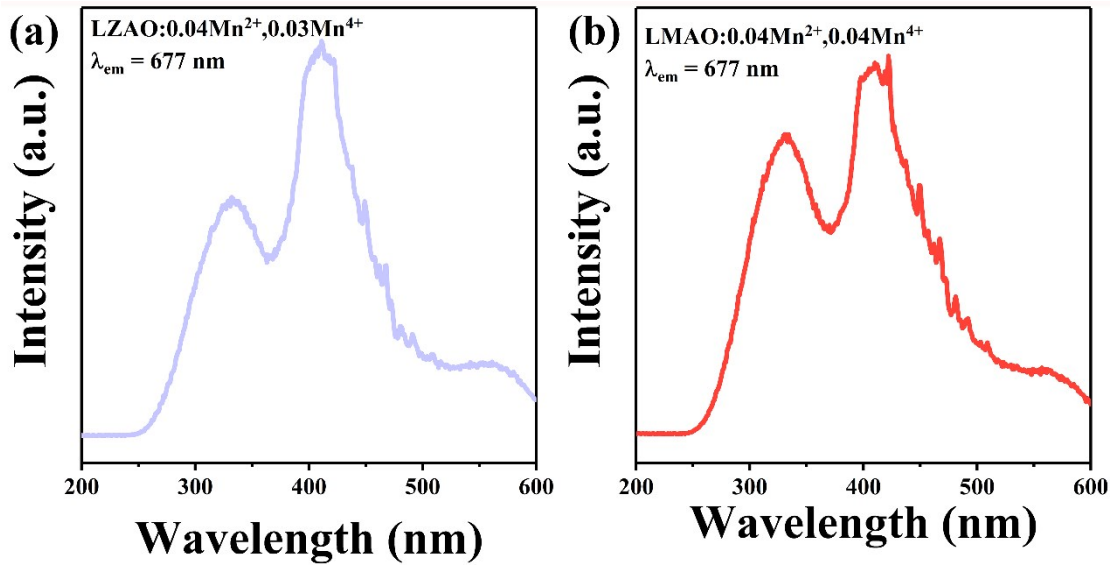

Figure S6. PLE of (a) LZAO:0.04Mn^{2+},0.03Mn^{4+} and (b) LMAO:0.04Mn^{2+},0.04Mn^{4+}sample (λ_{em} = 677 nm).

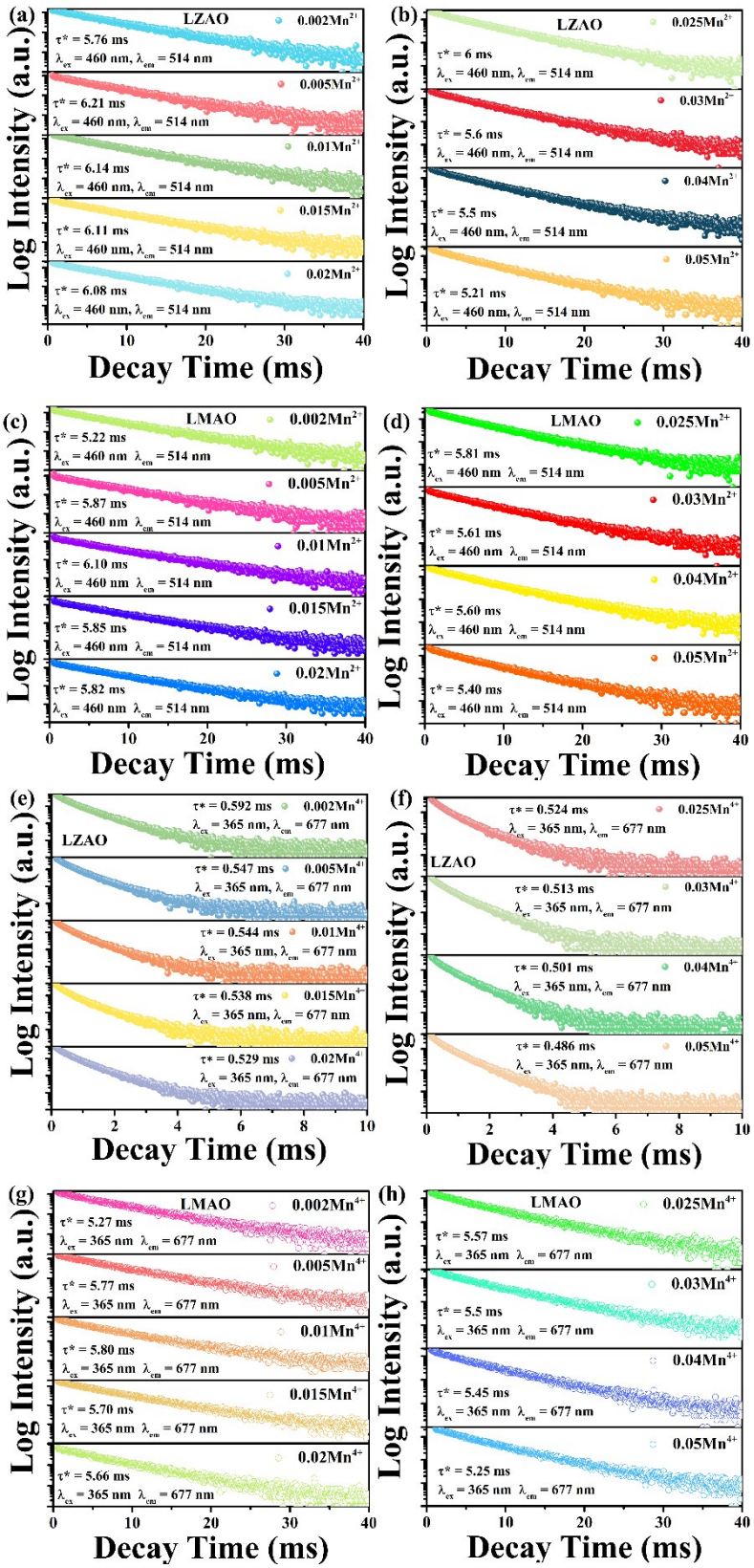

Figure S7. Decay curves of Mn^{2+} in (a-b) $LaZnAl_{11}O_{19}$:$x$$Mn^{2+}$ and (c-d) $LaMgAl_{11}O_{19}$:$x$$Mn^{2+}$ (λ_{ex} = 460 nm, λ_{em} = 514 nm). PL decay curves of Mn^{4+} in (e-f) $LaZnAl_{11}O_{19}$:$y$$Mn^{4+}$ and (g-h) $LaMgAl_{11}O_{19}$:$y$$Mn^{4+}$ (λ_{ex} = 365 nm, λ_{em} = 677 nm).

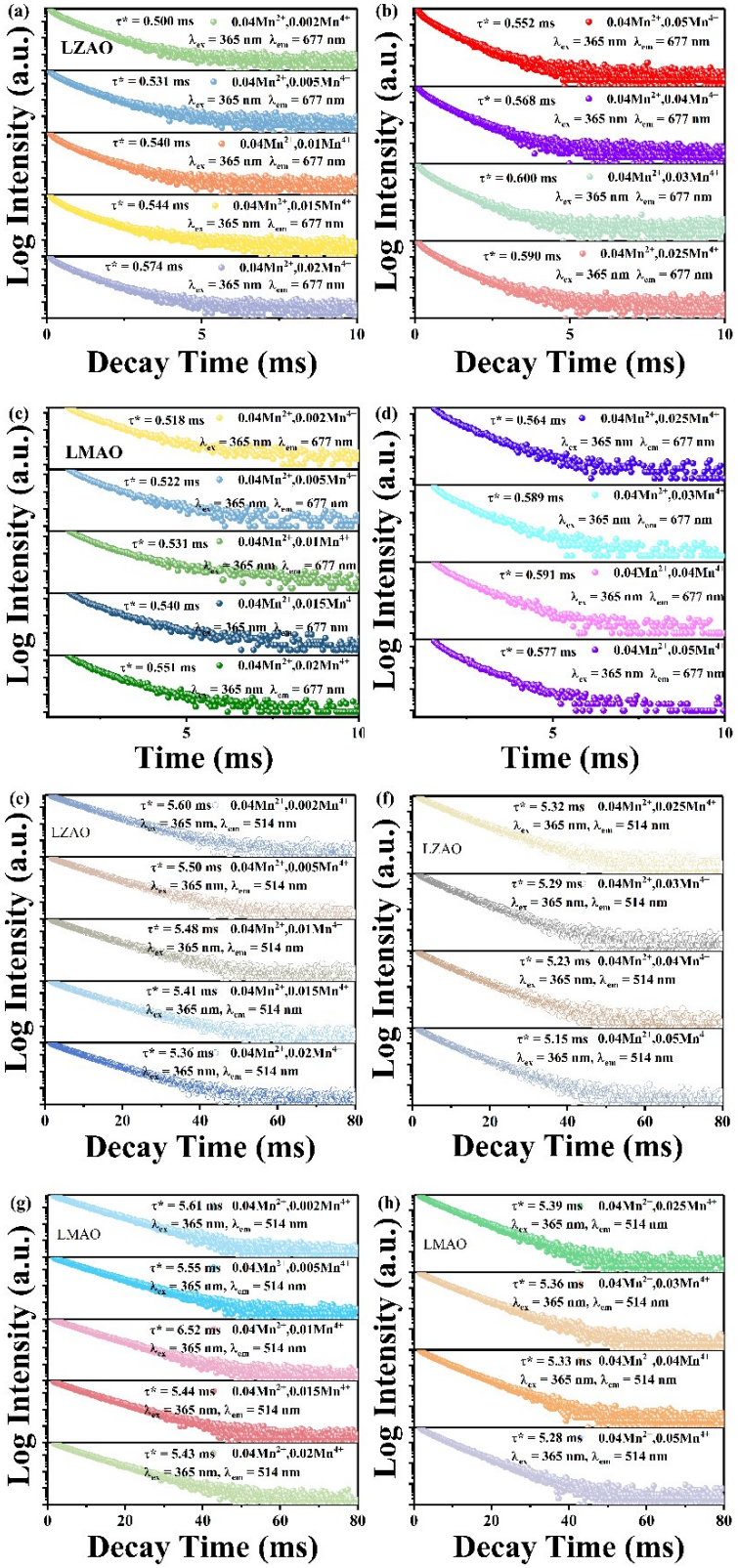

Figure S8. Decay curves of Mn^{4+} in (a-b) $LaZnAl_{11}O_{19}$:$0.04Mn^{2+}$,yMn^{4+} and (c-d) $LaMgAl_{11}O_{19}$:$0.04Mn^{2+}$,yMn^{4+}(λ_{ex} = 365 nm, λ_{em} = 677 nm). Decay curves of Mn^{2+} in (e-f) $LaZnAl_{11}O_{19}$:$0.04Mn^{2+}$,yMn^{4+} and (g-h) $LaMgAl_{11}O_{19}$:$0.04Mn^{2+}$,yMn^{4+}(λ_{ex} = 365 nm, λ_{em} = 514 nm).

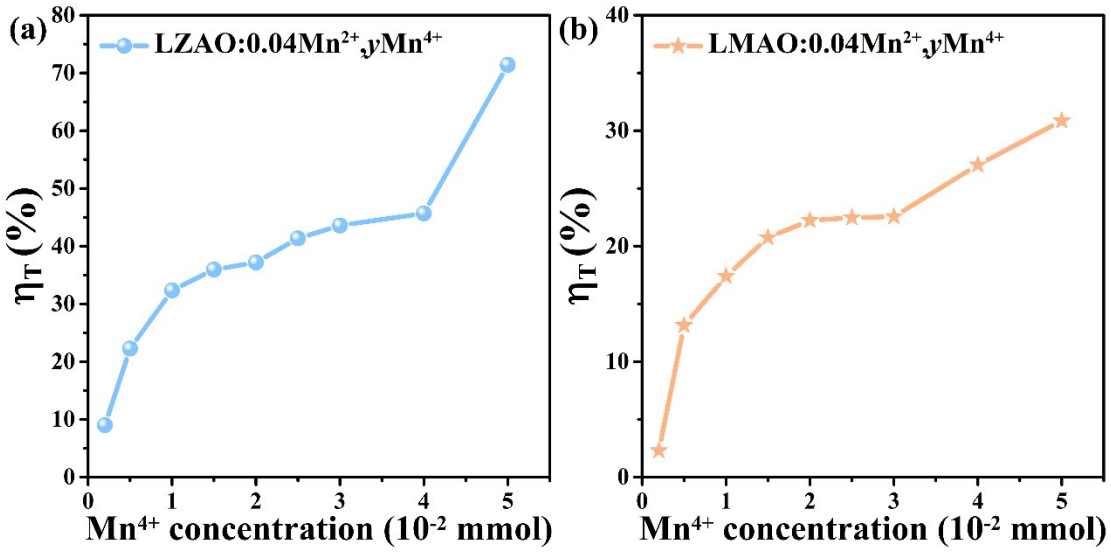

Figure S9. (a-b) Dependence of energy transfer efficiencies (η_T) on Mn^{4+} concentration in $LaM_{1-x}Al_{11-y}O_{19}$:0.04Mn^{2+},yMn^{4+} (M = Mg, Zn) phosphors.

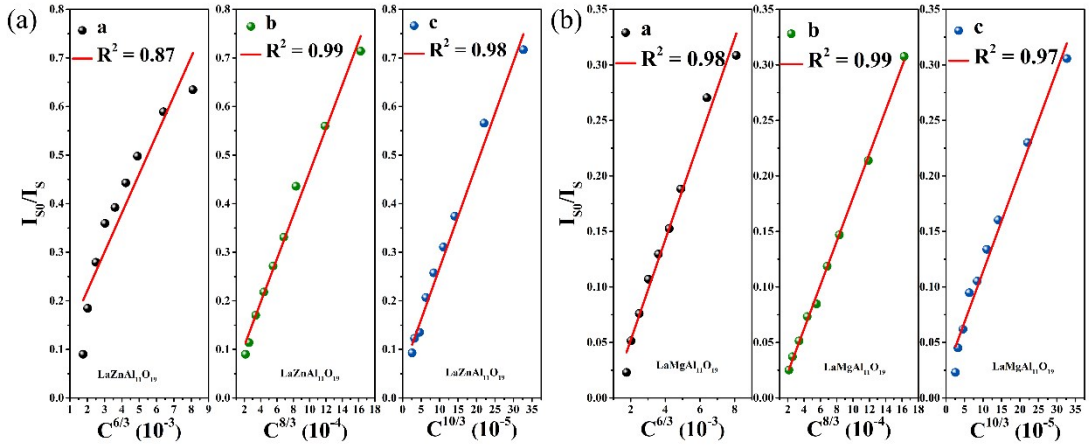

Figure S10. (a-b) Dependence of I_{S0}/I_S of Mn^{2+} on $C^{6/3}$, $C^{8/3}$ and $C^{10/3}$ in $LaM_{1-x}Al_{11-y}O_{19}$:0.04Mn^{2+},$y$$Mn^{4+}$ (M = Mg, Zn).

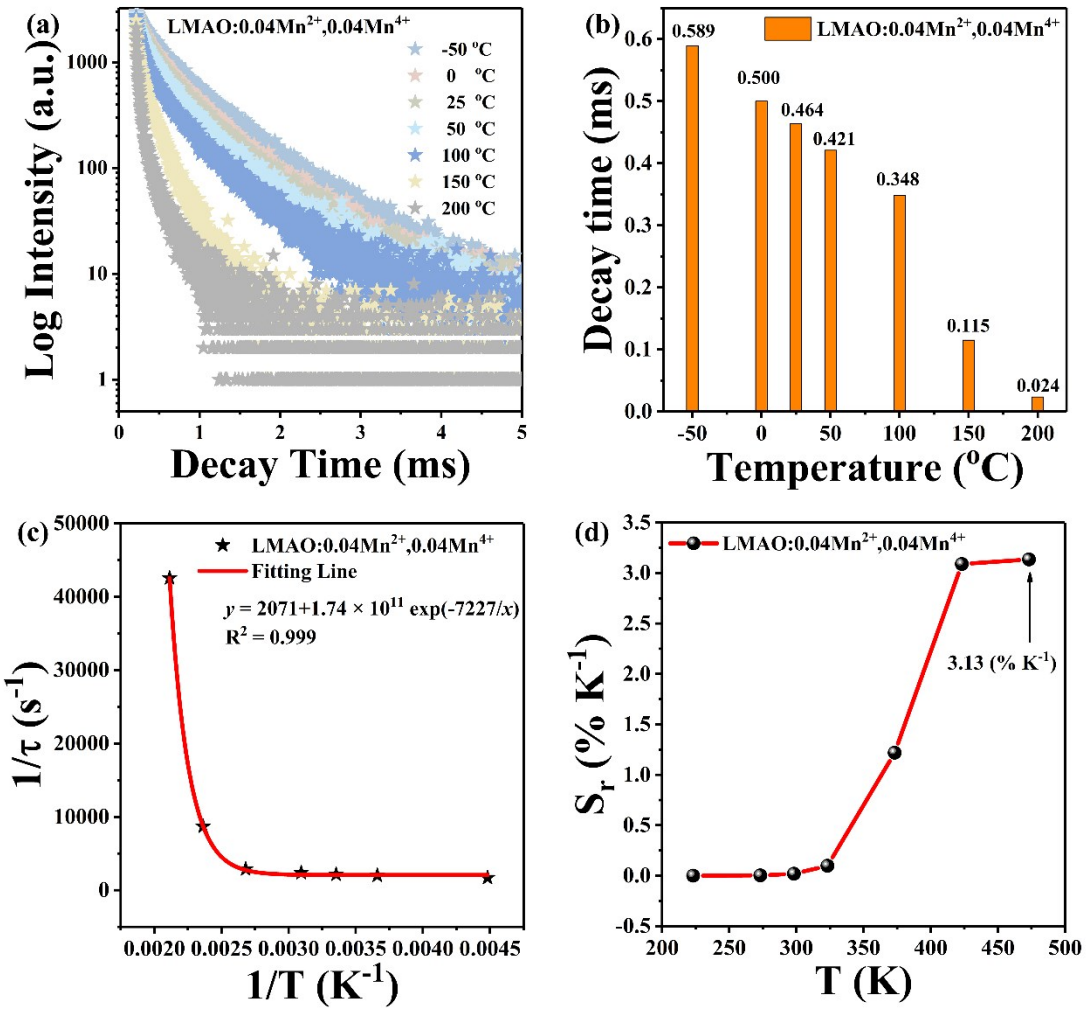

Figure S11. (a) Decay curves of $LaMgAl_{11}O_{19}$:0.04Mn^{2+},0.04Mn^{4+} in -50~200 °C. (b) Changing tendency of the fitted decay lifetimes with temperature. (c) Correlation between 1/τ vs 1/T and the exponential fitting line. (d) Calculated S_r $LaMgAl_{11}O_{19}$:0.04Mn^{2+},0.04Mn^{4+} temperature probe derived from lifetime readout in -50~200 °C.

Table S1. Refined crystallographic data and reliability factor for $LaMAl_{11}O_{19}$:0.04Mn^{2+},0.03Mn^{4+}/0.04Mn^{4+} (M = Mg, Zn).

formula	symmetry	Space group	a=b/Å	c/Å	V/Å	Z	R_{wp} (%)	R_p (%)
$LaZnAl_{11}O_{19}$	Hexagonal	P63/mmc	5.59	21.96	594.3	2	7.4	8.6
$LaMgAl_{11}O_{19}$	Hexagonal	P63/mmc	5.57	21.93	589.2	2	6.9	7.5

Table S2. The CIE coordinates of the $LaMAl_{11}O_{19}:0.04Mn^{2+},0.03Mn^{4+}/0.04Mn^{4+}$ (M = Mg, Zn) at different temperatures.

Temperature (°C)	$LaZnAl_{11}O_{19}:0.04Mn^{2+},0.03Mn^{4+}$		$LaMgAl_{11}O_{19}:0.04Mn^{2+},0.04Mn^{4+}$	
	x	*y*	*x*	*y*
-175	0.46	0.45	0.43	0.45
-100	0.40	0.50	0.40	0.47
-50	0.37	0.51	0.38	0.50
0	0.34	0.55	0.37	0.52
50	0.30	0.58	0.35	0.55
100	0.28	0.60	0.32	0.57
150	0.25	0.62	0.29	0.60
200	0.21	0.64	0.25	0.65
250	0.16	0.67	0.19	0.70